Investigation on an innovative resorption system for seasonal thermal energy storage

L. Jiang[a,b,*], R.Z. Wang[a], L.W. Wang[a], A.P. Roskilly[b]

[a] *Institute of Refrigeration and Cryogenics, Shanghai Jiao Tong University, Shanghai, 200240, China*

[b] *Sir Joseph Swan Centre for Energy Research, Newcastle University, Newcastle NE1 7RU, UK*

Abstract: An innovative resorption system is established and investigated for seasonal thermal energy storage. Solar energy is stored in form of chemical potential in summer whereas the stored energy could be released in form of sorption heat in winter. Working pair of $MnCl_2$-$CaCl_2$-NH_3 is selected and composite sorbents are developed with expanded natural graphite treated with sulfuric acid as the matrix for heat and mass transfer intensification. It is indicated that the highest effective heat storage density, heat power density and system *COP* are able to reach 1047 $kJ \cdot kg^{-1}$, 402 $W \cdot kg^{-1}$ and 0.58 under the condition of 30°C heat output temperature and 15°C ambient temperature. Novel resorption thermal energy storage system verifies the feasibility for seasonal energy storage at high ambient temperature in winter, which reveals great potentials for solar energy utilization. Also worth noting that two possible solutions i.e. temperature upgrade mode and sorption-compression mode are analyzed and compared when ambient temperature is relatively low i.e. below 0°C. Results demonstrate that heat could be supplied in term of -15°C ambient temperature and 50°C heat output temperature. Two methods could deal with the issues at low ambient temperature, which have their respective advantages for different applications.

Keywords: Resorption; Seasonal thermal energy storage; Solar energy; Composite sorbent

** Corresponding author. Tel. +86-21-34206309*

Email: maomaojianglong@sjtu.edu.cn (L. Jiang)

Nomenclature

c	Specific heat ($kJ \cdot kg^{-1} \cdot K^{-1}$)
COP	Coefficient of performance
ENG-TSA	Expanded natural graphite treated with sulfuric acid
ENG	Expanded natural graphite
EHSD	Effective heat storage density ($kJ \cdot kg^{-1}$)
HSD	Heat storage density ($kJ \cdot kg^{-1}$)
HPD	Heat power density ($W \cdot kg^{-1}$)
HTS	High temperature salt
h	Enthalpy ($kJ \cdot kg^{-1}$)
LTS	Low temperature salt
M	Mass (kg)
m	Mass flow rate ($kg \cdot s^{-1}$)
P	Pressure (Pa)
PCM	Phase change material
Q	Heat (kJ)
R	Gas constant ($J \cdot mol^{-1} \cdot K^{-1}$)
RTES	Resorption thermal enery storage
STES	Sorption thermal energy storage
T	Temperature (^oC)
TES	Thermal enery storage

Greek letters

ΔH	Enthalpy of sorbent

Subscripts

a	Ambient
c	Condensation
d	Desorption
discha	Discharging
e	Electricity
eq	Equilibrium

h	High
i	Inlet
in	Input
l	Low
m	Mass
o	Outlet
out	Output
R	Reaction
re	Recovery
s	Sorption
sen	Sensible
sor	Sorbent
up	Upgrade

1. Introduction

As a typical type of renewable energy, solar energy is characterized as discontinuity and instability due to the fact that solar insolation varies with weather condition, location, time and season of a year[1]. To deal with these disadvantages, thermal energy storage (TES) has been considered a possible solution to solar energy utilization by adjusting time-discrepancy, space-discrepancy and instability between energy supplies and demands [2-4]. Consequently, advanced solar TES technology has drawn burgeoning attentions in recent years.

Solar TES could be generally classified into short term and long term energy storage which is determined by the length of storage period. As a representative long term energy storage method, seasonal energy storage is of great significance since solar heat could be stored in summer and used in winter, which is much different from short term storage to transfer the heat from daytime to the night. It is extensively acknowledged that a common solar sensible heat storage product i.e. hot water tank has the disadvantages of large volume and heat loss, which is only suitable for short term solar energy storage. Another solar storage product is phase change material (PCM) tank [5, 6]. Although system mass and volume are reduced, it still takes a risk of releasing its stored energy ahead of time, which will result in large heat loss during the storage phase. To seek for an efficient seasonal solar energy

storage technology has become an urgent challenge, which is required to avoid heat loss during long storage period by using low-cost and reliable materials. Compared with conventional sensible and latent heat storage, sorption thermal energy storage (STES) has the advantages of high energy storage density, stable output temperature and good capability of both short term and long term energy storage[7]. Also worth noting that flexible working modes of STES could be realized, which are namely direct heat supply[8], cold and heat cogeneration to supply useful cold and heat simultaneously[9] as well as energy upgrade to upgrade the quality of thermal energy[10]. The external heat source promotes the decomposition of sorption work pair, and energy could be stored in forms of chemical potentials separately. When sorbate and sorbent come to react again, heat will be released in exothermic process[11]. In this process, energy could then be stored without heat loss as long as sorbent and sorbate are kept separate[12]. In spite of these distinguished traits, it is admitted that liquid ammonia inside the evaporator of STES system will result in safety risk if high heat output temperature is required. An improved safety and system compactness could be obtained by resorption thermal energy storage (RTES) since there is no liquid ammonia in the system. Evaporator/condenser is replaced by LTS reactor[13].

With regard to both STES and RTES, heat input and output power rate are usually considered as two key parameters, which are closely relevant with sorption characteristics. It is extensively acknowledged that granular metal halides will have the disadvantages of swelling and agglomeration, which will reduce sorption and desorption rate. Composite sorbent is regarded as a common solution due to the improved thermal conductivity and permeability [14, 15]. Expanded natural graphite(ENG)[15, 16], carbon nanoparticle[17], aluminum and vermiculite[18] have been investigated as the matrix for heat and mass transfer enhancement. Various working pairs could be selected for STES and RTES, which are mainly determined by working temperature ranges and external demands[19]. Among them, $CaCl_2$-NH_3 working pair has been widely investigated not only for STES, but also for air conditioner and ice maker due to its thermal and sorption stability[20]. For utilization of medium temperature heat source, $MnCl_2$-NH_3 is another good selection for seasonal solar TES due to its proper desorption and sorption temperature [21]. With regard to RTES, $MnCl_2$ is often selected as high temperature salt (HTS) whereas various low temperature salts (LTSs) such as NH_4Cl, $CaCl_2$, $SrCl_2$, NaBr and $BaCl_2$ etc. are investigated for best match[22, 23]. $MnCl_2$-$CaCl_2$-NH_3 working pair has been extensively analyzed due to its good performance and system reliability[24]. In our previous work,

different working modes of RTES system by using $MnCl_2$-$CaCl_2$-NH_3 have been investigated and compared i.e. direct heat supply, cold and heat cogeneration as well as energy upgrade. Nonetheless, these all belongs to researches of short term energy storage. In fact, long term or seasonal thermal energy storage is completely a different scenario which may demonstrate different working performance since sensible heat will have a negative effect.

This paper aims to investigate the performance of RTES system for seasonal energy storage. Heat storage density and system efficiency are evaluated and compared under the condition of different heat input, heat output and ambient temperatures. Also worth noting that two possible approaches for seasonal energy storage are analyzed and compared at low ambient temperature in winter, which verifies their feasibilities and respective advantages.

2. RTES for seasonal energy storage

Fig.1 indicates schematic diagram of RTES for seasonal energy storage, which is composed of HTS and LTS sorption reactor. An insulation layer will be placed to avoid mutual heat loss. Two reactors are connected with a channel and a refrigerant valve. During the charging process in summer as shown in Fig.1a, HTS reactor is heated by external heat source i.e. solar energy. Refrigerant is desorbed from HTS reactor to LTS reactor, and LTS reactor releases sorption heat $Q_{s,LTS}$ to environmental heat sink. After the charging process, refrigerant valve between HTS and LTS reactor will be closed to separate resorption working pair. Thermal energy will be stored and transformed in form of chemical potential. Once heat is required in winter as shown in Fig.1b, refrigerant valve between HTS and LTS reactor will be opened again. Since HTS and LTS reactor are at ambient temperature in the initial stage of discharging process, HTS reactor will first be heated from ambient temperature to heat output temperature by sorbing the refrigerant from LTS reactor. Desorption heat $Q_{d,LTS}$ is taken away by environmental heat sink while effective heat output of HTS reactor will be used for end user.

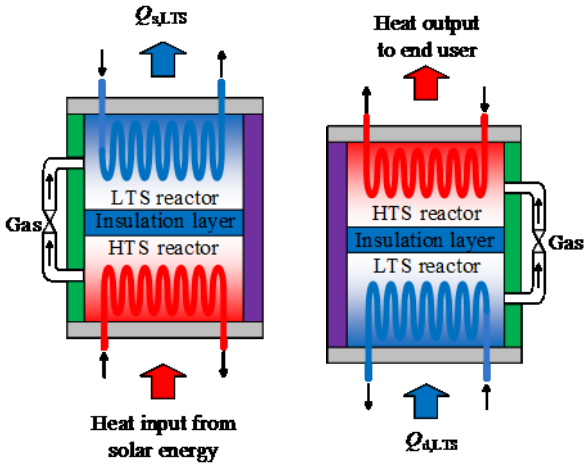

(a) (b)

Fig.1. Schematic diagram of RTES for seasonal energy storage (a) charging process; (b) discharging process.

Table 1 shows the main parameters of selected metal halides. Equilibrium reaction lines are calculated by equation (1). To simplify the description of thermochemical reaction processes of different metal halides, phrases of $MnCl_2$ 6/2, $CaCl_2$ 8/4, $CaCl_2$ 4/2 are used in the paper, which could be referred to our previous work[19]. For example, $MnCl_2$ 6/2 represents the process in which $MnCl_2$ ammoniate reacts with ammonia from 2 moles to 6 moles. Also worth noting that $CaCl_2$ proceeds two reaction processes of $CaCl_2$ 8/4 and $CaCl_2$ 4/2 in selected working temperature range. Chemical reaction equations between $MnCl_2$, $CaCl_2$ and ammonia could be referred to equation (2)-(5).

$$\mathrm{Ln}(P_{\mathrm{eq}}) = -\frac{\Delta H_{\mathrm{R}}}{RT_{\mathrm{eq}}} + \frac{\Delta S}{R} \tag{1}$$

$$\mathrm{MnCl_2 \cdot 2NH_3 + 4NH_3 \leftrightarrow MnCl_2 \cdot 6NH_3} + 4\Delta H_{\mathrm{MnCl_2}} \tag{2}$$

$$\mathrm{CaCl_2 \cdot 2NH_3 + 2NH_3 \leftrightarrow CaCl_2 \cdot 4NH_3} + 2\Delta H_{\mathrm{CaCl_2}} \tag{3}$$

$$\mathrm{CaCl_2 \cdot 4NH_3 + 4NH_3 \leftrightarrow CaCl_2 \cdot 8NH_3} + 4\Delta H_{\mathrm{CaCl_2}} \tag{4}$$

$$\mathrm{NH_3(gas) \leftrightarrow NH_3(liq)} + \Delta H_{\mathrm{c}} \tag{5}$$

115 Table 1. The main parameters of selected metal halides[25].

Sorbent	Equilibrium desorption temperature (°C)	Reaction enthalpy ($J \cdot mol^{-1}$)	Maximum cycle sorption quantity ($kg \cdot kg^{-1}$)	Energy density ($kJ \cdot kg^{-1}$)
$MnCl_2$ 6/2	152	47416	0.54	1509
$CaCl_2$ 4/2	97	42269	0.31	763
$CaCl_2$ 8/4	86	41403	0.61	1481

116

117 Fig.2 indicates *P-T* diagram of RTES for seasonal energy storage, in which Fig.2a shows general
118 schematic diagram whereas Fig.2b demonstrates *P-T* diagram by using $MnCl_2$-$CaCl_2$-NH_3 working pair.
119 Since $CaCl_2$ will eventually proceed the reaction from 4 mol to 8 mol in selected working range,
120 reaction line of $CaCl_2$ 4/2 isn't indicated in Fig.2b. During the charging process in summer, HTS
121 reactor i.e. $MnCl_2$-ammoniate will be heated by solar energy Q_{in} at an input temperature of 85°C.
122 Ammonia will be desorbed from HTS reactor and flow into LTS reactor. LTS reactor will sorb the
123 refrigerant by rejecting sorption heat $Q_{s,LTS}$ to heat sink at a temperature of 30°C. Desorption process of
124 HTS reactor undergoes from point A to point B. In this process, thermal energy is converted into
125 chemisorption potential by breaking the binding force of resorption working pair. Refrigerant valve
126 between HTS and LTS reactor won't be opened until released heat is required. During the discharging
127 process in winter, both HTS and LTS reactor will be connected for chemical reaction. Ammonia will be
128 desorbed and then sorbed by HTS reactor. Sorption process will proceed from point C to point D. Most
129 of sorption heat Q_{out} released by HTS reactor is used to supply useful heat for end user at a temperature
130 of 55°C when ambient temperature is 5°C.

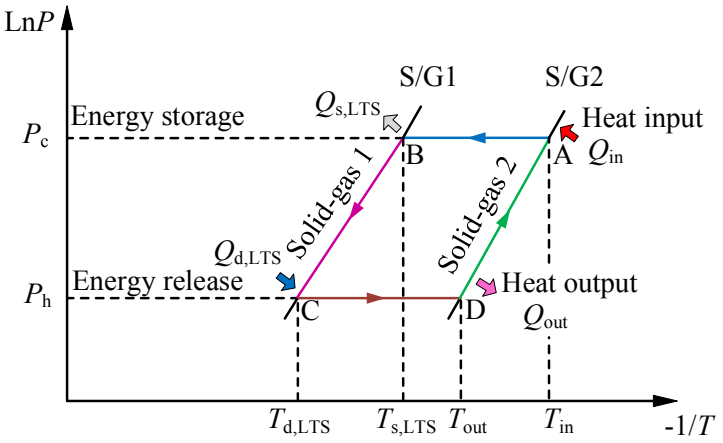

(a)

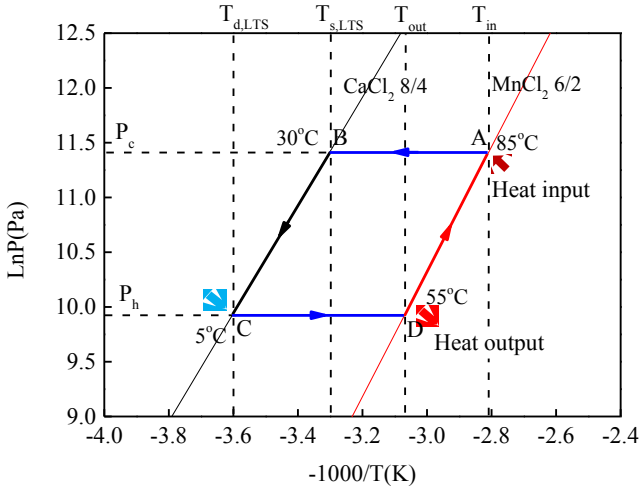

(b)

Fig.2. *P-T* diagram of RTES for seasonal energy storage (a) schematic; (b) $MnCl_2$-$CaCl_2$-NH_3.

Fig.3 indicates the photo of RTES system for seasonal energy storage, which is composed of HTS and LTS reactor, pressure gauge, ammonia valve and auxiliary equipment. HTS and LTS reactor consists of three unit fin tube sorption reactors, respectively. HTS and LTS reactor are filled with 4.9 kg composite $MnCl_2$ and 3.8 kg composite $CaCl_2$. Composite sorbents are developed with ENG-TSA as the matrix for heat and mass transfer intensification[26]. The developing procedures of composite sorbents can be referred to the reference[27]. Composite sorbents are impregnated with ENG-TSA as a mass ratio of 6:1 which are squeezed into fin gaps of finned tubes. The auxiliary equipment mainly includes a water thermostat, a cooling tower, an oil tank, pressure sensors, flowmeters, temperature

sensors and a data collector. Oil tank controls the temperature of HTS reactor which is used to simulate external heat source as solar energy in summer. Water thermostat is used to control the temperature of LTS reactor. In the experiment, flowrate of oil and water are about 1.4 $m^3 \cdot h^{-1}$ and 0.9 $m^3 \cdot h^{-1}$, respectively. Pressure sensors (full scale from 0 to 2.5 MPa with tolerance of ±0.1%) are placed at HTS and LTS reactor. Pt100 thermal resistance temperature sensors with 0.2% accuracy are adopted to measure inlet and outlet temperatures of HTS and LTS reactors. The experimental data are monitored and logged by an Agilient 34972A data collector.

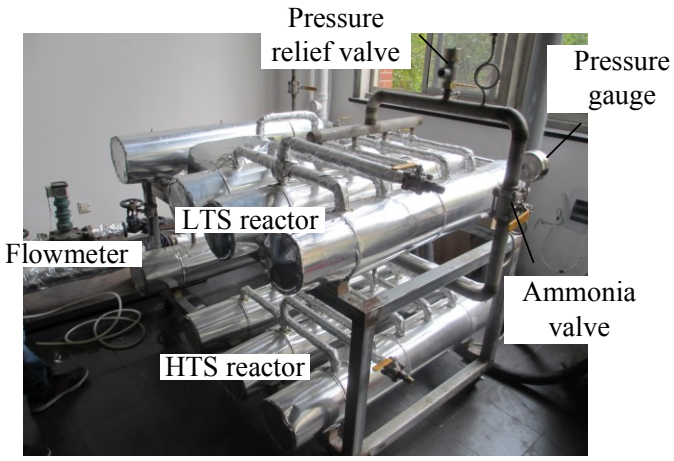

Fig.3. RTES system for seasonal energy storage.

For this experiment, charging and discharging process will be operated every other day to ensure that temperatures of HTS and LTS before discharging process are the same with ambient temperature. To comprehensively investigate the performance of RTES system for seasonal energy storage, different heat input and output temperatures are adopted for comparison. Heat input temperature ranges from 130°C to 150°C with the increment of 10°C whereas heat output temperature is selected from 30°C to 50°C. Heat input temperature is in the temperature range of solar collector which should also be higher than equilibrium desorption temperature of $MnCl_2$. Heat output temperature could be used for hot water supply, low-temperature radiant floor heating system and small temperature difference fan-coil unit. Also worth noting that ambient temperature of the experiment ranges from 5°C to 15°C, which is

determined by local temperature in winter. Due to the limitation of local temperature and sorption characteristics, performance of RTES system for seasonal energy storage could not be directly investigated in term of low ambient temperature i.e. below 0°C. Two possible solutions will be analyzed and compared based on testing data to verify their feasibilities.

3. Performance evaluation

Heat input of RTES system for seasonal energy storage during the charging process can be expressed as equation (6):

$$Q_{\text{in}} = \int_0^{t_{\text{in}}} c_{\text{o}} \cdot m_{\text{o}} \cdot \left(T_{\text{HTS,i}} - T_{\text{HTS,o}}\right) \mathrm{d}t \tag{6}$$

where Q_{in} is total heat input during the charging process, which is composed of desorption heat, sensible heat consumed by composite sorbent and metal of HTS reactor. t_{in} is time for heat input of HTS reactor. m_{o} is mass flow rate of oil. C_{o} is specific heat of oil. $T_{\text{HTS,i}}$ and $T_{\text{HTS,o}}$ are inlet and outlet temperature of HTS reactor.

Heat output of RTES system for seasonal energy storage during the discharging process can be expressed as equation (7)-(9):

$$Q_{\text{discha}} = \int_0^{t_{\text{discha}}} c_{\text{oil}} \cdot m_{\text{oil}} \cdot \left(T_{\text{HTS,i}} - T_{\text{HTS,o}}\right) \mathrm{d}t \tag{7}$$

$$Q_{\text{out}} = Q_{\text{discha}} - Q_{\text{sen}} \tag{8}$$

$$Q_{\text{sen}} = c_{\text{oil}} \cdot m_{\text{oil}} \cdot \left(T_{\text{out}} - T_{\text{a}}\right) \tag{9}$$

where Q_{discha} is total heat output during the discharging process. Q_{out} is effective heat output for end user. Q_{sen} is sensible heat consumption of HTS reactor. t_{discha} is time for heat output of HTS reactor.

Mass heat storage density HSD_{m} and effective mass heat storage density can be expressed as equation (10)-(11):

$$HSD_m = \frac{Q_{\text{dischar}}}{\text{M}_{\text{sor}}} \tag{10}$$

$$EHSD_m = \frac{Q_{\text{out}}}{\text{M}_{\text{sor}}} \tag{11}$$

where M_{sor} is mass of HTS and LTS composite sorbent.

Heat power density HPD_{m} can be expressed as equation (12):

$$HPD_m = \frac{Q_{\text{out}}}{t_{\text{discha}} \cdot \text{M}_{\text{sor}}} \tag{12}$$

Heat storage efficiency *COP* can be expressed as equation (13):

$$COP = \frac{Q_{\text{out}}}{Q_{\text{in}}} \tag{13}$$

4. Results and discussions

4.1 Temperature and pressure variation for seasonal energy storage

Temperature and pressure of sorption system for seasonal energy storage are considered as two key factors, which could be used for revealing the characteristics of RTES. It is also regarded as important composition for clear elaborating novelty of the system for seasonal energy storage since there is few research work about ammonia RTES prototype.

Since temperatures of HTS and LTS reactor under different working conditions show similar trends, 150^{o}C input temperature in summer and 10^{o}C ambient temperature in winter are selected and investigated as a representative working condition, which is shown in Fig.4. HTS and LTS reactor are first controlled at 25^{o}C ambient temperature. Afterwards, HTS reactor will be heated by oil of 150^{o}C, which is simulated as external heat source. Inlet and outlet temperature of HTS reactor increase remarkably as shown in Fig.4a. The highest system pressure is 0.82 MPa during the charging process as shown in Fig.4b. The desorption process of HTS reactor is controlled in 30 minutes due the fact that reaction is almost complete and heat power rate will be reduced with excessive time. Then, ammonia valve is closed to separate HTS and LTS reactor. Thermal energy is transformed and stored in the form of chemical bonds during the charging process.

During the discharging process, HTS and LTS reactor are cooled down to 10^{o}C ambient temperature in winter after seasonal storage period due to inevitable heat losses between energy storage unit and external environment. When the stored thermal energy is required to be released for meeting heat demand of end user, ammonia valve will be opened and sorption process of HTS reactor occurs. A small part of sorption heat will be consumed for heating HTS reactor to heat output temperature of

50°C, then heat transfer fluid will flow into the reactor for transporting the heat released. It is indicated that sorption heat produced by HTS reactor is almost used to supply heat for end user at a heat output temperature higher than 50°C. Simultaneously, desorption heat of LTS rector is consumed by external heat sink at an ambient temperature of 10°C. Also worth noting that outlet temperature of HTS reactor is always higher than its inlet temperature due to sorption heat, and the highest temperature difference between inlet and outlet temperature of HTS reactor is as high as 9.3°C during the discharging process.

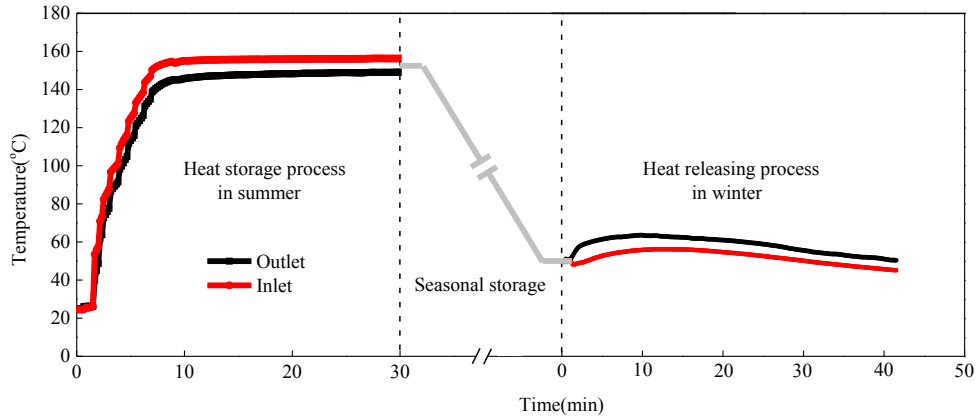

(a)

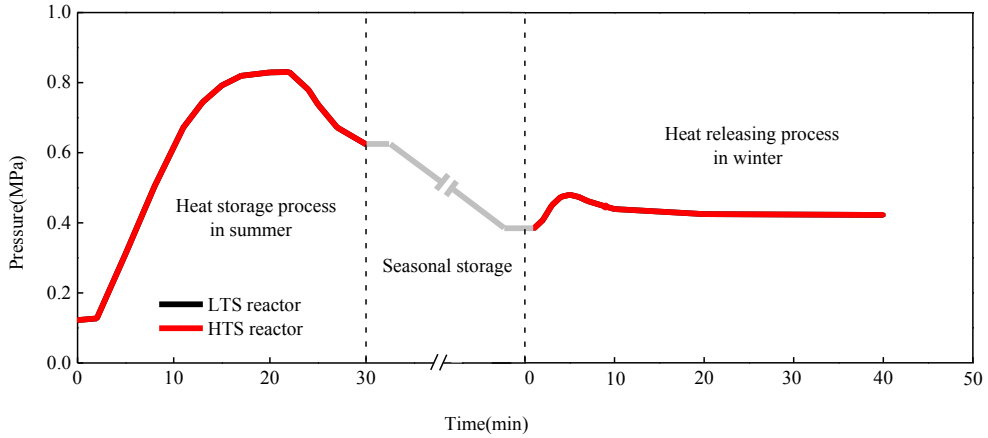

(b)

Fig.4. Temperature and pressure in the charging and discharging process for seasonal energy storage (a) inlet and outlet temperature of HTS reactor; (b) pressure.

4.2 Heat storage density and system *COP*

For evaluating the performance during the discharging process, heat storage density and effective heat storage density for seasonal energy storage are evaluated according to equation (10) and (11). The former is to investigate ideal heat output with regard to only sorption heat, and the latter is to assess the effective heat output by considering both sorption heat and sensible heat consumed by the reactor. Fig.5 indicates mass heat storage density under different heat output temperatures, heat input temperatures and ambient temperatures. Fig.5a demonstrates that mass heat storage density increases with the decrease of heat output temperature and the increase of ambient temperature. This is mainly because that the higher output temperature will result in the increase of heat loss to the environment. Another reason is that the higher ambient temperature and lower heat output temperature will lead to larger chemical potential, which accelerates sorption reaction rate during the discharging process. Fig.5b shows that mass heat storage density increases with the increase of heat input temperature. Also worth noting that mass heat storage density is more sensitive to heat input temperature rather than ambient temperature. The highest mass heat storage density is able to reach 1149 $kJ \cdot kg^{-1}$ under the condition of 150°C heat input temperature, 15°C ambient temperature and 30°C heat output temperature. For different working conditions, mass heat storage density ranges from 646 $kJ \cdot kg^{-1}$ to 1149 $kJ \cdot kg^{-1}$.

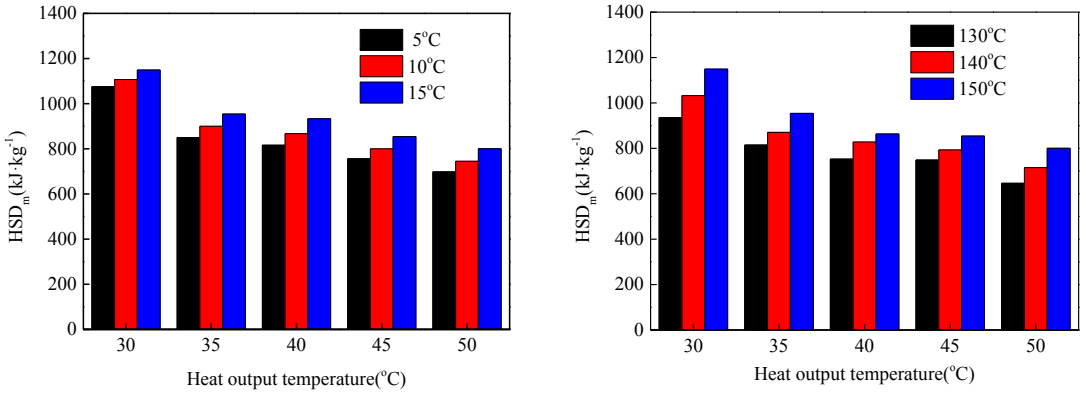

(a) (b)

247 Fig.5. Heat storage density of RTES for seasonal energy storage vs. (a) ambient temperature; (b) heat
248 input temperature.

249

250 Fig.6 shows effective mass heat storage density with regard to real heat output. Compared with
251 mass heat storage density, effective heat storage density declines remarkably due to additional sensible
252 heat consumption of HTS reactor. It is worth noting that effective heat storage density is influenced by
253 both chemical reaction potential and sensible heat of the reactor. Effective heat storage density also
254 increases with the increase of heat input temperature and the decease of heat output temperature, which
255 has a larger increment than that of heat storage density. The highest effective mass heat storage density
256 is able to reach 1047 $kJ \cdot kg^{-1}$ under the same condition of 150°C heat input temperature, 15°C ambient
257 temperature and 30°C heat output temperature. For different working conditions, effective heat storage
258 density ranges from 398 $kJ \cdot kg^{-1}$ to 1047 $kJ \cdot kg^{-1}$.
259

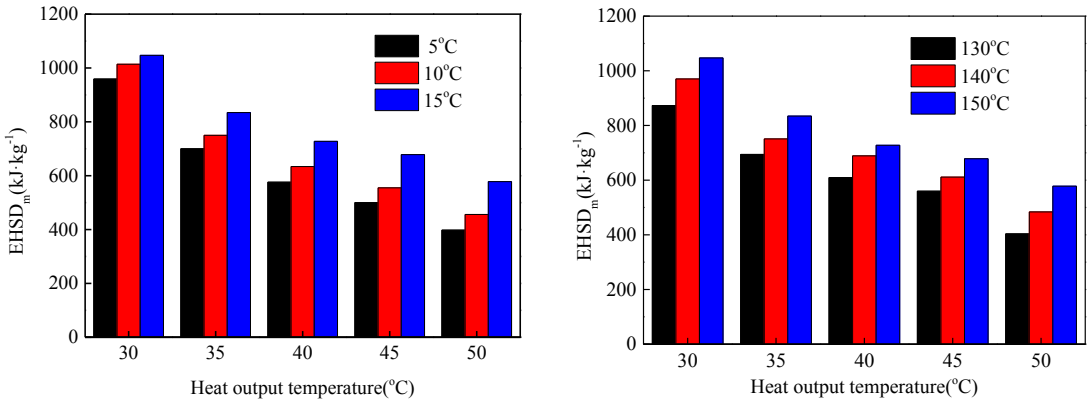

(a) (b)

260 Fig.6. Effective heat storage density of RTES for seasonal energy storage vs. (a) ambient temperature;
261 (b) heat input temperature.

In some cases, capacity and time of heat output should be considered to meet the demands of end users. Heat power density is defined and used to assess heat discharging rate of RTES system for seasonal energy storage, which is shown in Fig.7. The lower heat output temperature results in higher heat power density. For different heat output temperatures and ambient temperatures, heat power density ranges from 180 $W \cdot kg^{-1}$ to 402 $W \cdot kg^{-1}$ when heat input temperature is 150°C. Besides, system *COP* for heat output is related with effective heat output during the discharging process in winter and heat input during the charging process in summer. Fig.8 demonstrates system *COP* under the condition of 150°C heat input temperature, 30-50°C heat output temperatures and 5-15°C ambient temperatures. The highest system *COP* is 0.58 when heat output and ambient temperature are 30°C and 15°C. For different heat output and ambient temperatures, system *COP* is in the range from 0.21 to 0.58.

Based on all the accuracies of measuring sensors, errors of heat storage density, heat storage density, heat power density and COP of RTES system for seasonal energy storage are 4.5%, 5.1%, 5.2% and 5.8%, respectively.

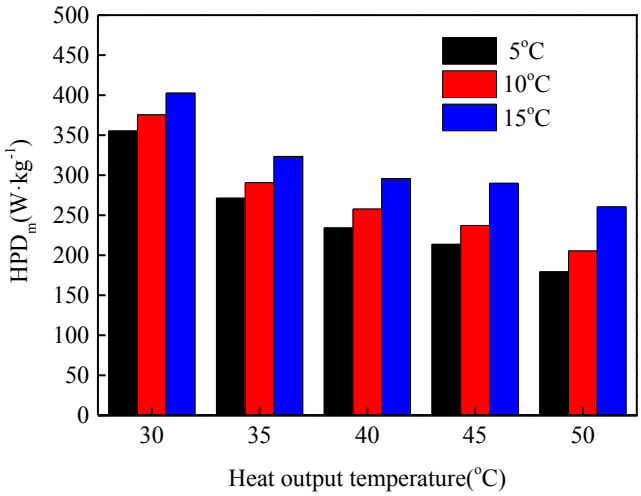

Fig.7. Heat power density of RTES system for seasonal energy storage.

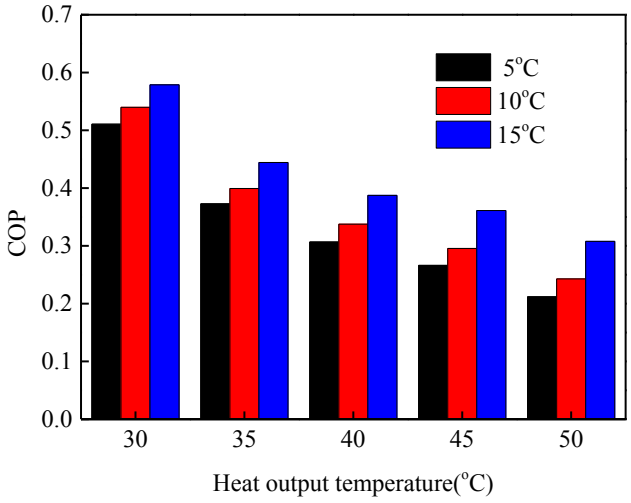

Fig.8. System *COP* of RTES system for seasonal energy storage.

It is widely acknowledged that sensible heat of metal part could be used to supply the heat for end user when considering short-term energy storage. For long-term or seasonal energy storage, sensible heat could not be utilized and even have a negative effect on heat output by consuming part of sensible heat at the initial stage of discharging process. Mass ratio between metal and composite sorbent is used to evaluate the influence of sensible heat consumption on system *COP*. For theoretical thermal analysis of RTES system, mass ratio between metal and sorbent is usually assumed as 1. However, for real system this ratio cannot be reached by constraints of manufacture processing and cost. One remarkable fact is that mass ratio of STES system is generally higher than that of RTES due to the fact that condenser/evaporate will be calculated into the mass of whole system. Considering RTES system for seasonal energy storage in this experiment, mass ratio between metal and sorbent is still as high as 5.9. Fig.9 indicates system performance of RTES system in term of different mass ratios, which is used to further investigate the potential improvement. It is worth noting that system *COP* could be improved by reducing the mass of metal part of RTES system.

When mass of metal part isn't taken into account, the highest *COP* is able to reach 0.763 under the condition of 150°C heat input temperature, 30°C heat input temperature and 15°C ambient temperature.

Nonetheless, the highest experimental system *COP* is only about 0.58. Except for sensible heat consumption of metal part, one main reason is that global conversion rate of RTES is lower than 1, which is defined as the percentage of composite sorbent that reacts with the refrigerant. Another reason is that heat dissipation of reactors in the charging and discharging process could not be neglected in a real system. Fig.9 also reveals great potentials to improve system efficiency by reducing mass ratio if global conversion rate isn't able to be further improved. For different heat output temperatures, system *COP* will be improved by up to 37% when mass ratio decreases from 5.9 to 3.

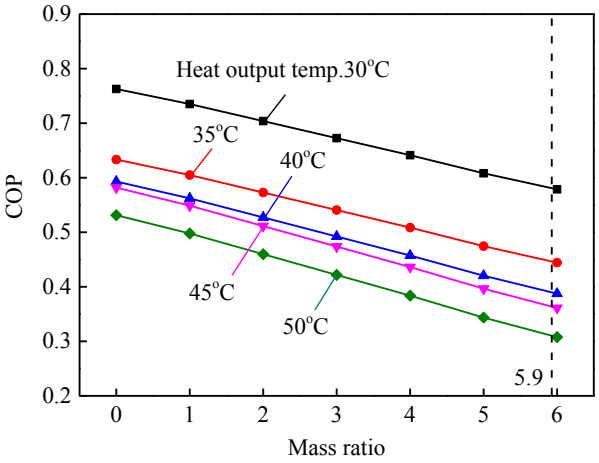

Fig.9. *COP* of RTES for seasonal energy storage vs. different mass ratios.

To further illustrate the novelty of sorption system for seasonal energy storage, the experimental system is compared with other sorption prototypes at high ambient temperature in term of storage method, operation condition, HSD and COP. Ambient temperature and output temperature of these systems are almost around 15°C and 40°C, which are shown in Table 2. Sensible and latent heat storage systems are not selected for comparison due to their low energy density and different applications.

One remarkable fact is that water is mainly used as working fluid of sorption systems for seasonal energy storage, and few researches of ammonia systems are reported for seasonal energy storage. It is indicated that this novel sorption system takes an advantage in HSD though it has a

relative low system COP, which proves that the system still has a reasonable performance at high ambient temperature. Also worth noting that water STES system could not realize energy storage when evaporation temperature is lower than 0°C. Comparably, ammonia system for seasonal energy storage could achieve that, which will be further analyzed in next section.

Table 2. Comparison of sorption prototypes by using different working pairs.

Storage method	Operation condition	HSD ($kJ \cdot kg^{-1}$)	COP	refs
Closed LiCl-water sorption	Charging temperature 85°C; Ambient temperature 15°C; Discharging temperature 40°C	500 (1 kW·h storage)	53%	[28]
Closed LiCl-water sorption	Charging temperature 87°C; Ambient temperature 15°C; Discharging temperature 25°C	648 (35 kW·h storage)	53%	[29]
Closed $SrBr_2$-water sorption	Charging temperature 85°C; Ambient temperature 15°C; Discharging temperature 40°C	455 (1 kW·h storage)	48%	[30]
Closed $SrBr_2$-water sorption	Charging temperature 80°C; Ambient temperature 15°C; Discharging temperature 35°C	486 (60 kW·h storage)	-	[31]
Closed zeolite-water sorption	Charging& Discharging temperature 180°C	514 (1 kW·h storage)	-	[29]
Closed silica gel-water sorption	Charging temperature 88°C; Ambient temperature 16°C; Discharging temperature 38°C	234 (13 kW·h storage)	50%-	[29]
Closed $MnCl_2$-$CaCl_2$ -ammonia sorption	Charging temperature 130°C; Ambient temperature 15°C; Discharging temperature 40°C	580 (1 kW·h storage)	45%	Present study

5. Possible solutions to low ambient temperature

5.1 Temperature upgrade mode

For low ambient temperature in winter, heat output temperature of RTES system could not reach the required demand through a set of HTS and LTS reactor due to the monovariant characteristic of chemisorption reaction. Under this scenario, one possible solution is temperature upgrade mode which

increases heat output temperature by using internal heat recovery between two sets of HTS and LTS reactors, which is similar with the method for STES[32].

Fig.10 indicates schematic diagram of temperature upgrade mode of RTES system for seasonal energy storage. Two sets of HTS and LTS reactors are integrated into one tank, and HTS reactor 1 is connected with LTS reactor 2 by thermal fluid pipe. Charging process in summer is similar with the situation as shown in Fig.1. During the discharging process with low ambient temperature in winter, sorption heat of HTS reactor 1 will be used to heat LTS reactor 2 to increase its working pressure, which will result in the higher heat output temperature of HTS reactor 2 to meet the required demands of end user.

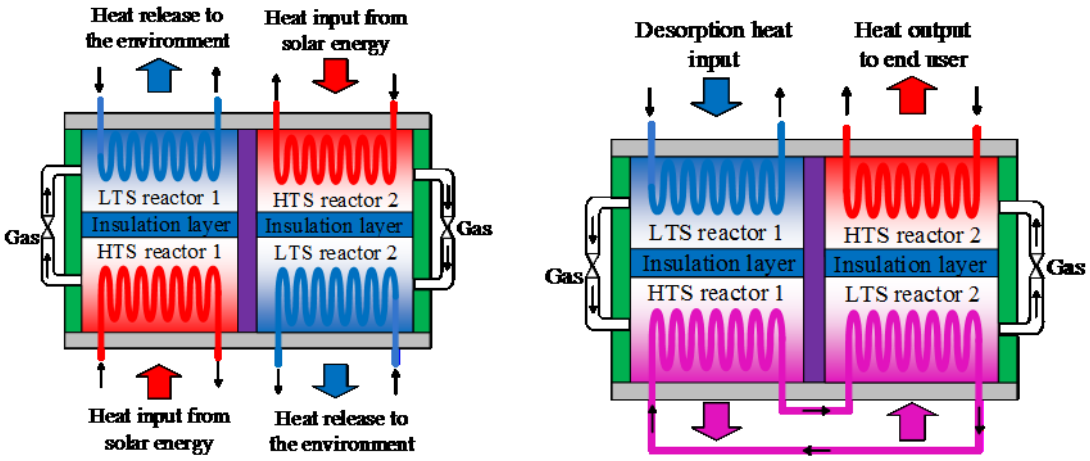

(a) (b)

Fig.10. Schematic diagram of RTES system for temperature upgrade mode (a) charging process; (b) discharging process.

Fig.11 indicates *P-T* diagram of RTES for seasonal energy storage with respect to low ambient temperature in winter. Fig.11a shows the general schematic whereas Fig.11b demonstrates *P-T* diagram by using $MnCl_2$-$CaCl_2$-NH_3 working pair. When ambient temperature is -20°C in winter, equilibrium

sorption temperature of $MnCl_2$ is 36°C for the reaction from $MnCl_2{\cdot}2NH_3$ to $MnCl_2{\cdot}6NH_3$. Heat output temperature is relatively low which may not meet some heating requirements of end user. In this case, temperature upgrade mode will be adopted to increase heat output temperature by using internal heat recovery between HTS reactor 1 and LTS reactor 2. Sorption reaction heat released by HTS reactor 1 at working pressure P_l (E-F) is recovered and used as a second heat source to supply the sensible and desorption heat of LTS reactor 2. LTS reactor 2 will be heated from ambient temperature of -20°C to a higher temperature of 5°C (E-C) to achieve temperature-upgrade sorption process. The ammonia could then be desorbed by LTS reactor 2 and flows to HTS reactor 2 to proceed sorption process at a high working pressure P_h (C-D). Sorption heat released by HTS reactor 2 is used to supply thermal energy for end user at a high temperature of 55°C.

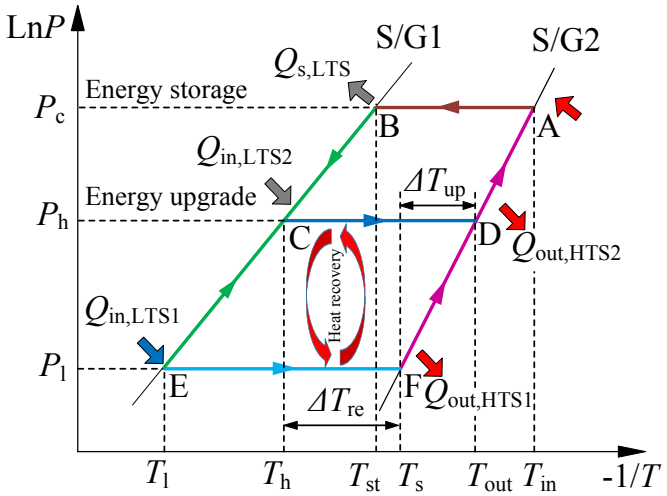

(a)

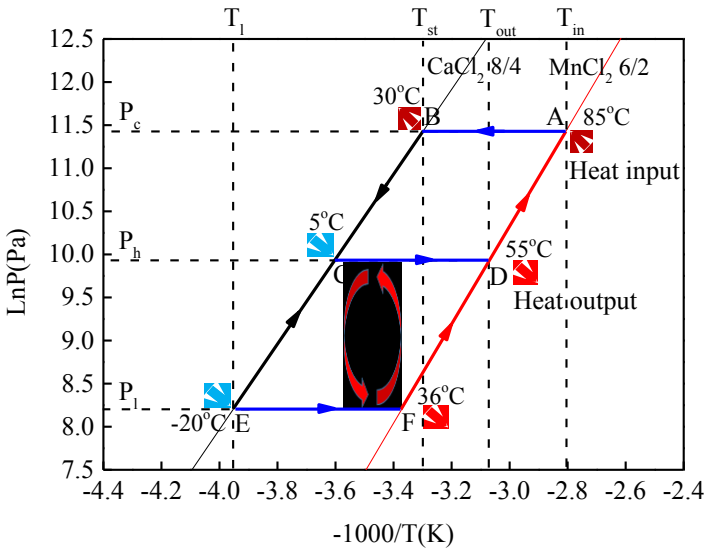

(b)

Fig.11. *P-T* diagram of RTES system for temperature upgrade mode (a) schematic; (b) $MnCl_2$-$CaCl_2$-NH_3.

Since there is only a set of HTS and LTS reactor of the experimental RTES system for seasonal energy storage, this section is to verify the feasibility of temperature upgrade mode. -15°C ambient temperature and 30°C heat output temperature are selected as one representative working condition for HTS and LTS reactor 1. Considering heat transfer temperature difference as 15°C, 15°C input temperature of LTS reactor 2 and 50°C heat output temperature of HTS reactor 2 are investigated for heat output of temperature upgrade mode. Since system performance for HTS and LTS reactor 2 under the selected condition has been evaluated above, the main work will focus on internal heat recovery. That is whether sorption heat released by HTS reactor 1 at a heat output temperature of 30°C is enough to be used to supply the required heat consumption of LTS reactor 2 to increase its working pressure. It is worth noting that sorption heat $Q_{s,HTS1}$ released by HTS reactor 1 is used to provide its sensible heat $Q_{sen,HTS1}$ with the temperature from -15°C to 30°C, sensible heat $Q_{sen,LTS2}$ of LTS reactor 2 from -15°C to

374 15°C and desorption heat $Q_{d,LTS2}$ of LTS reactor 2. Therefore, temperature upgrade mode of RTES for
375 seasonal energy storage will be feasible and valid only in the premise of equation (14), which could be
376 transformed to equation (16). Based on experimental results, $Q_{out,LTS1}$ is about 5365 kJ which is much
377 higher than $Q_{in,LTS2}$ of 3184 kJ. This demonstrates that HTS reactor 2 is able to produce heat at a
378 temperature of 50°C though ambient temperature is as low as -15°C in winter. Heat storage density and
379 system *COP* of temperature upgrade mode are also analyzed which are 578 kJ·kg^{-1} and 0.155
380 respectively under the condition of -15°C ambient temperature and 50°C heat output temperature.

381 $$Q_{s,HTS1} \geq Q_{sen,HTS1} + Q_{d,LTS2} + Q_{sen,LTS2} \quad (14)$$

382 $$Q_{s,HTS1} - Q_{sen,HTS1} \geq Q_{d,LTS2} + Q_{sen,LTS2} \quad (15)$$

383 $$Q_{out,HTS1} \geq Q_{in,LTS2} \quad (16)$$

384
385

386 **5.2 Sorption-compression mode**

387 Although temperature upgrade mode is able to solve the issue at low ambient temperature in
388 winter, two sets of HTS and LTS reactors are required which will inevitably result in low system
389 compactness. Another alternative solution i.e. sorption-compression mode is proposed to deal with low
390 ambient temperature in winter, which is shown in Fig.12. During the charging process, HTS and LTS
391 reactor operates similarly with the situation as shown in Fig.1. Different from temperature upgrade
392 mode above, a compressor is introduced to pressurize the desorbed ammonia, which is conducive to
393 sorption of HTS reactor and desorption of LTS reactor during the discharging process. A part of
394 electricity will be consumed when pressure potential between HTS and LTS reactor is not enough to
395 promote the reaction with regard to the required heat output temperature.

396

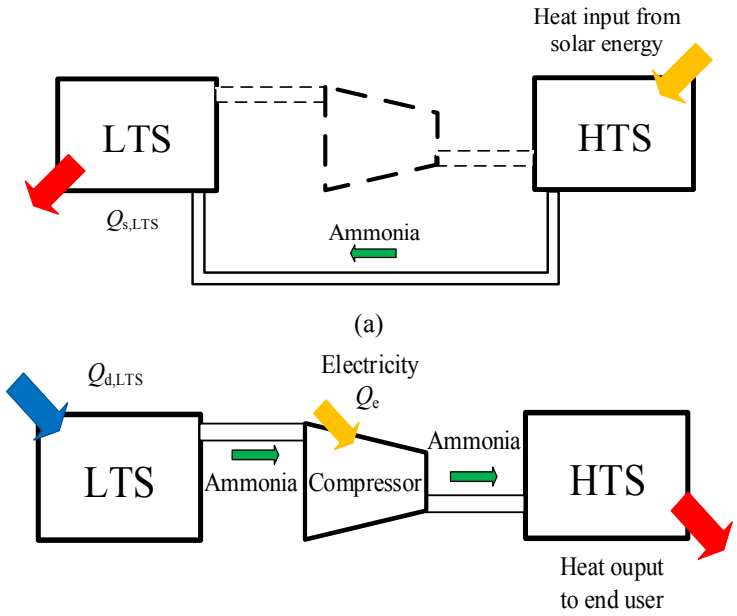

Fig.12. Schematic diagram of RTES system for sorption-compression mode (a) charging process; (b) discharging process.

Fig.13 indicates *P-T* diagram of RTES system for seasonal energy storage when ambient temperature is relatively low. Fig.13a shows the general schematic whereas Fig.13b demonstrates *P-T* diagram by using $MnCl_2$-$CaCl_2$-NH_3 working pair. It is indicated that the closed cycle A-B-E-F could be realized when ambient temperature is low, and output temperature T_s is 36°C which may not meet the requirements. Under this scenario, novel cycle A-B-E-C-D is proposed to increase heat output temperature, which is described as follows: During the charging process, HTS reactor will be heated by solar thermal energy with input temperature 85°C. Ammonia will be desorbed from HTS reactor and flows into LTS reactor. LTS reactor will sorb the refrigerant by rejecting sorption heat to heat sink at a temperature of 30°C. Desorption process will proceed from point A to point B. During the discharging process, LTS reactor undergoes decomposition at point E at ambient temperature of -20°C, the desorbed ammonia vapor afterwards is pressurized in an isentropic compression process from E to

point C to achieve the equilibrium reaction pressure of HTS reactor. Since it is not straight line for this isentropic process thermodynamically, the dotted line is used which demonstrates the schematic process. Ammonia is eventually sorbed by HTS reactor at point D to supply the required output heat with temperature 55°C.

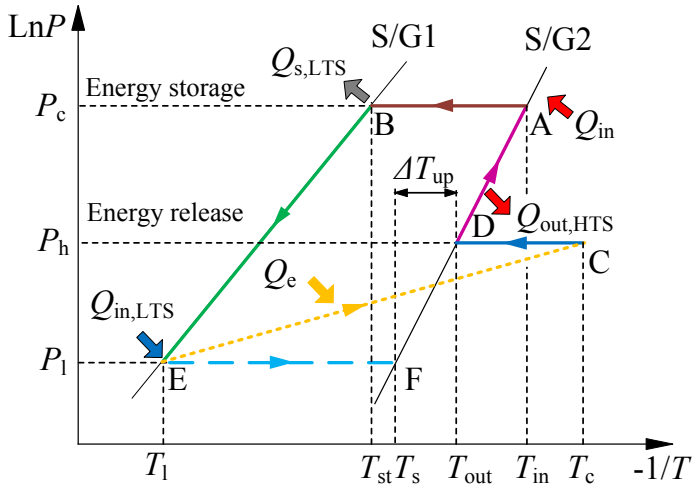

(a)

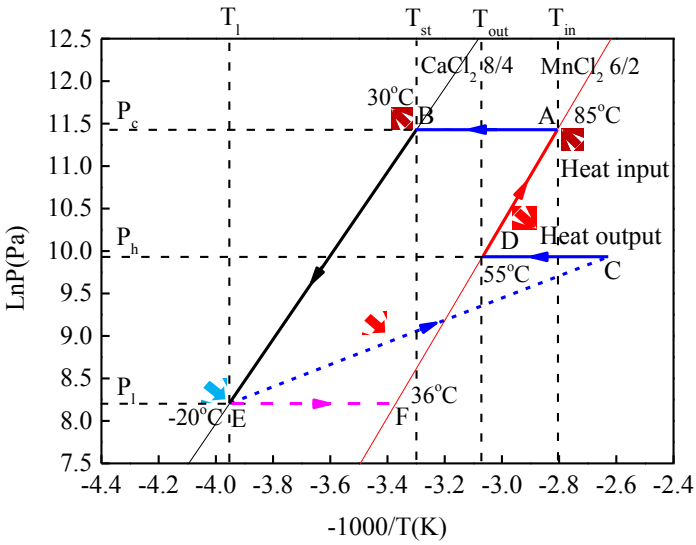

(b)

Fig.13. *P-T* diagram of RTES system for sorption-compression mode (a) schematic; (b) $MnCl_2$-$CaCl_2$-NH_3.

To further make a comparison between temperature upgrade mode and sorption-compression mode, one representative working condition for seasonal energy storage i.e. 50^{o}C output temperature and -20^{o}C ambient temperature is selected in term of different system parameters and performance. The isentropic compression efficiency is assumed as 0.8. It is noting that external conditions i.e. output temperature and ambient temperature in winter will not change the compared system characteristic, which indicates qualitative analysis for these two working modes.

Advantages and disadvantages of temperature upgrade mode and sorption-compression mode are evaluated as shown in Table 3, which will be further elaborated for real application. It is demonstrated that sorption-compression mode has a higher system compactness than that of temperature upgrade mode. This is mainly because the former consists of one set of HTS and LTS reactor whereas the latter has two sets of HTS and LTS reactors. Thus temperature upgrade mode isn't always suitable for small-scale application with limited volume and mass. Considering energy input, only heat is required for temperature upgrade mode. Comparably, both electricity and heat are required for sorption-compression mode, which may not be applied for the place where no extra electricity could be supplied. Since compressor is introduced to RTES system, thermal and mechanical stability of sorption-compression mode will be reduced. Also worth noting that effective energy storage densities of two working modes are quite similar whereas system COP of sorption-compression mode is much higher than that of temperature upgrade mode due to the fact that heat input will be double for two sets of HTS and LTS reactors. RTES system with sorption-compression mode will be more flexible to external working conditions with a larger working range and improved performance by consuming a small part of electricity.

Table 3. Comparisons of two possible solutions to low ambient temperature.

Mode	System compactness	Energy input	Mechanical Stability	Thermal Stability	*EHSD* ($kJ \cdot kg^{-1}$)	*COP*
Temperature upgrade	Low	Heat	High	High	578	0.155
Sorption-compression	Moderate	Heat &Power	Moderate	Moderate	590	0.258

6. Conclusions

An innovative RTES system for seasonal energy storage is established, and working pair of $MnCl_2$-$CaCl_2$-NH_3 is selected. Different heat input temperatures, ambient temperatures and heat output temperatures are adopted to investigate the overall system performance. Besides, two possible solutions are evaluated and compared with regard to relatively low ambient temperature. Conclusions are yielded as follows:

(1) Mass heat storage density and effective mass heat storage density increase with the increase of ambient temperature. The highest mass heat storage density and effective mass heat storage density are able to reach 1149 $kJ \cdot kg^{-1}$ and 1047 $kJ \cdot kg^{-1}$ under the condition of 150°C heat input temperature, 15°C ambient temperature and 30°C heat output temperature. For different working conditions, mass heat storage density and effective mass heat storage density range from 646 $kJ \cdot kg^{-1}$ to 1149 $kJ \cdot kg^{-1}$ and from 398 $kJ \cdot kg^{-1}$ to 1047 $kJ \cdot kg^{-1}$, respectively.

(2) The lower heat output temperature results in the higher heat power density. Heat power density ranges from 180 $W \cdot kg^{-1}$ to 402 $W \cdot kg^{-1}$ when heat input temperature is 150°C. The highest system *COP* is 0.58 when heat output and ambient temperature are 30°C and 15°C. For different heat output and ambient temperatures, system *COP* ranges from 0.21 to 0.58. System *COP* will be improved by up to 37% when mass ratio decreases from 5.9 to 3.

(3) Two possible approaches of RTES system for seasonal energy storage are analyzed and

compared to solve the issue at low ambient temperature in winter. It is worth noting that RTES system with temperature upgrade mode has better thermal and mechanical stability which is suitable for the place where no extra electricity could be supplied. Comparably, system with sorption-compression mode will be more flexible to external working conditions. An improved system performance could be accomplished with a small part of electricity input with regard to sorption-compression mode.

With the potentially wide use of thermal energy storage technology, RTES technology for seasonal energy storage could be considered as an alternative method for further utilization of solar energy. Performance of RTES system is used to verify the feasibility for seasonal energy storage at low ambient temperature by using two possible solutions, which demonstrates their flexibility and adaptability to severe working conditions.

Acknowledgements: This research was supported by National Natural Science Foundation of China under contract number (51606118), foundation for Innovative Research Groups of National Natural Science Foundation of China (51521004) and Heat-STRESS project (EP/N02155X/1) funded by Engineering and Physical Science Research Council of the UK.

References

[1] Rashidi S, Esfahani JA, Rashidi A. A review on the applications of porous materials in solar energy systems. Renewable and Sustainable Energy Reviews. 2017;73:1198-210.

[2] Cot-Gores J, Castell A, Cabeza LF. Thermochemical energy storage and conversion: A-state-of-the-art review of the experimental research under practical conditions. Renewable and Sustainable Energy Reviews. 2012;16(7):5207-24.

[3] Balasubramanian G, Ghommem M, Hajj MR, Wong WP, Tomlin JA, Puri IK. Modeling of

494 thermochemical energy storage by salt hydrates. International Journal of Heat and Mass Transfer.
495 2010;53(25–26):5700-6.
496 [4] Lovegrove K, Luzzi A, Soldiani I, Kreetz H. Developing ammonia based thermochemical energy
497 storage for dish power plants. Solar Energy. 2004;76(1–3):331-7.
498 [5] Ghoreishi-Madiseh SA, Sasmito AP, Hassani FP, Amiri L. Performance evaluation of large scale
499 rock-pit seasonal thermal energy storage for application in underground mine ventilation. Applied
500 Energy. 2017;185, Part 2:1940-7.
501 [6] Xu J, Wang RZ, Li Y. A review of available technologies for seasonal thermal energy storage. Solar
502 Energy. 2014;103:610-38.
503 [7] N'Tsoukpoe KE, Liu H, Le Pierrès N, Luo L. A review on long-term sorption solar energy storage.
504 Renewable and Sustainable Energy Reviews. 2009;13(9):2385-96.
505 [8] Jiang L, Zhu FQ, Wang LW, Liu CZ, Wang RZ. Experimental investigation on a $MnCl_2$-$CaCl_2$-NH_3
506 thermal energy storage system. Renewable Energy. 2016;91:130-6.
507 [9] Zhu FQ, Jiang L, Wang LW, Wang RZ. Experimental investigation on a $MnCl_2$-$CaCl_2$-NH_3
508 resorption system for heat and refrigeration cogeneration. Applied Energy. 2016;181:29-37.
509 [10] Jiang L, Wang L, Wang R, Zhu F, Lu Y, Roskilly AP. Experimental investigation on an innovative
510 resorption system for energy storage and upgrade. Energy Conversion and Management.
511 2017;138:651-8.
512 [11] Freni A, Maggio G, Sapienza A, Frazzica A, Restuccia G, Vasta S. Comparative analysis of
513 promising adsorbent/adsorbate pairs for adsorptive heat pumping, air conditioning and refrigeration.
514 Applied Thermal Engineering. 2016;104:85-95.
515 [12] Scapino L, Zondag HA, Van Bael J, Diriken J, Rindt CCM. Sorption heat storage for long-term

516 low-temperature applications: A review on the advancements at material and prototype scale. Applied
517 Energy. 2017;190:920-48.
518 [13] Cabeza LF, Solé A, Barreneche C. Review on sorption materials and technologies for heat pumps
519 and thermal energy storage. Renewable Energy. 2017;110:3-39.
520 [14] Han JH, Lee KH. Gas permeability of expanded graphite–metallic salt composite. Applied
521 Thermal Engineering. 2001;21(4):453-63.
522 [15] Jiang L, Wang LW, Jin ZQ, Wang RZ, Dai YJ. Effective thermal conductivity and permeability of
523 compact compound ammoniated salts in the adsorption/desorption process. International Journal of
524 Thermal Sciences. 2013;71:103-10.
525 [16] Jiang L, Wang LW, Wang RZ. Investigation on thermal conductive consolidated composite $CaCl_2$
526 for adsorption refrigeration. International Journal of Thermal Sciences. 2014;81:68-75.
527 [17] Yan T, Li TX, Li H, Wang RZ. Experimental study of the ammonia adsorption characteristics on
528 the composite sorbent of $CaCl_2$ and multi-walled carbon nanotubes. International Journal of
529 Refrigeration. 2014;46:165-72.
530 [18] Veselovskaya JV, Tokarev MM, Grekova AD, Gordeeva LG. Novel ammonia sorbents ‘‘porous
531 matrix modified by active salt” for adsorptive heat transformation: 6. The ways of adsorption dynamics
532 enhancement. Applied Thermal Engineering. 2012;37:87-94.
533 [19] Wang LW, Wang RZ, Oliveira RG. A review on adsorption working pairs for refrigeration.
534 Renewable and Sustainable Energy Reviews. 2009;13(3):518-34.
535 [20] Wang K, Wu JY, Wang RZ, Wang LW. Composite adsorbent of CaCl2 and expanded graphite for
536 adsorption ice maker on fishing boats. International Journal of Refrigeration. 2006;29(2):199-210.
537 [21] Sharma R, Kumar EA. A Comparative Thermodynamic Analysis of Gas–Solid Sorption System

538 Based On H2–La0.9Ce0.1Ni5/LaNi4.7Al0.3 and NH3–NaBr/$MnCl_2$. Energy Procedia.
539 2017;109:48-55.
540 [22] Bao HS, Oliveira RG, Wang RZ, Wang LW, Ma ZW. Working pairs for resorption refrigerator.
541 Applied Thermal Engineering. 2011;31(14–15):3015-21.
542 [23] Jiang L, Wang L, Roskilly AP, Wang R. Design and performance analysis of a resorption
543 cogeneration system. International Journal of Low-Carbon Technologies. 2013;8:85-91.
544 [24] Gao P, Wang LW, Wang RZ, Zhang XF, Li DP, Liang ZW, et al. Experimental investigation of a
545 $MnCl_2/CaCl_2$-NH_3 two-stage solid sorption freezing system for a refrigerated truck. Energy.
546 2016;103:16-26.
547 [25] Jiang L, Wang LW, Zhou ZS, Zhu FQ, Wang RZ. Investigation on non-equilibrium performance of
548 composite adsorbent for resorption refrigeration. Energy Conversion and Management.
549 2016;119:67-74.
550 [26] Wang LW, Metcalf SJ, Critoph RE, Thorpe R, Tamainot-Telto Z. Development of thermal
551 conductive consolidated activated carbon for adsorption refrigeration. Carbon. 2012;50(3):977-86.
552 [27] Jiang L, Wang LW, Luo WL, Wang RZ. Experimental study on working pairs for two-stage
553 chemisorption freezing cycle. Renewable Energy. 2015;74:287-97.
554 [28] Yu N, Wang RZ, Wang LW. Theoretical and experimental investigation of a closed sorption
555 thermal storage prototype using LiCl/water. Energy. 2015;93, Part 2:1523-34.
556 [29] Bales C. Laboratory tests of chemical reactions and prototype sorption storage units. 2008;Task
557 32.
558 [30] Zhao YJ, Wang RZ, Zhang YN, Yu N. Development of $SrBr_2$ composite sorbents for a sorption
559 thermal energy storage system to store low-temperature heat. Energy. 2016;115, Part 1:129-39.

560 [31] Mauran S, Lahmidi H, Goetz V. Solar heating and cooling by a thermochemical process. First
561 experiments of a prototype storing 60kWh by a solid/gas reaction. Solar Energy. 2008;82(7):623-36.
562 [32] Li T, Wang R, Kiplagat JK, Kang Y. Performance analysis of an integrated energy storage and
563 energy upgrade thermochemical solid–gas sorption system for seasonal storage of solar thermal energy.
564 Energy. 2013;50:454-67.
565
566